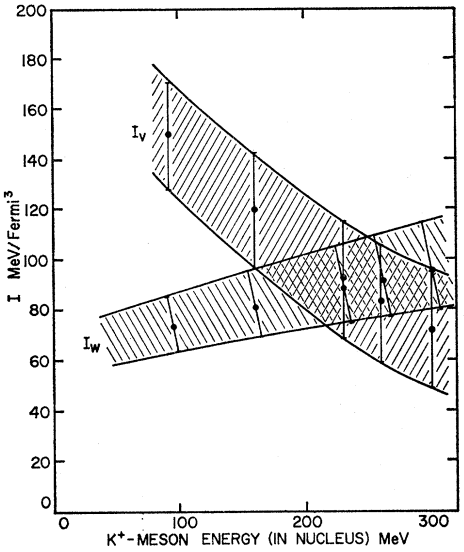

FIG. 4. The values of I_v and I_w predicted by the Stenger-Goldhaber phase shifts, as a function of energy. The points are energies that were explicitly calculated. The two bands contain all potential values that are allowed by the phase shifts.

for most radius parameters. The agreement with I_w is especially good—all radius parameters giving the value of I_w within the limits of error except for the extreme values of $R_0=1.07$ F and $a=0.20$ F taken together. If $a=0.20$ F, R_0 apparently should be more than 1.20 F; if R_0 is 1.07 F, a must be 0.5 F or more.

The analysis probably should not be extended much beyond 300 MeV as the d-wave phase shifts in the $T=0$ state and the p-wave phase shifts in the $T=1$ state will probably appear with significant strength at higher energies.

5. COMPARISON WITH PREVIOUS WORK

At lower energies, there have been two determinations of optical-model potentials for K^+ mesons from complex nuclei which can be directly compared with our analysis as they were obtained in an identical manner. At 93 MeV Melkanoff *et al.*[13] have obtained 123 ± 26 MeV-F^3 and 56 ± 8 MeV-F^3 for I_v and I_w, respectively, which agree reasonably well with the predictions from the directly determined phase shifts of 149 ± 22 and 73_{-11}^{+12} MeV-F^3. The agreement at 230 MeV between the potentials obtained by Melkanoff *et al.*[1] and Helmy *et al.*[6] and those predicted is also reasonable. These authors obtained $I_v=123\pm44$ MeV-F^3 and $I_w=103\pm13$ MeV-F^3, whereas the Stenger-Goldhaber phase shifts predict 93 ± 23 and 91_{-15}^{+18} MeV-F^3, respectively.

In conclusion, we may say that the agreement between the direct and indirect methods of obtaining the optical-model potentials is satisfactory and well within the error limits. It will be useful to repeat the calculation when the errors on the phase shifts have been reduced significantly.

ACKNOWLEDGMENTS

We are greatly indebted to Dr. E. Lofgren for Bevatron exposure facilities. We acknowledge the very great help of Miss Carol Boz, Rafe Sandes, and Dr. M. Taherzadeh in this work. Dr. M. A. Melkanoff gave unstintingly of his time in helping with the computer codes. We also thank Miss E. Conradie, Miss D. van Greunen, and P. Horn for their able assistance with the scanning.

[13] M. A. Melkanoff, O. R. Price, D. H. Stork, and H. K. Ticho, Phys. Rev. **113**, 1303 (1958).

PHYSICAL REVIEW VOLUME 138, NUMBER 6B 21 JUNE 1965

Photodisintegration of the Deuteron by Polarized Photons*

F. F. LIU
High-Energy Physics Laboratory, Stanford University, Stanford, California
(Received 12 February 1965)

The asymmetry in the photodisintegration of the deuteron by polarized photons has been measured between photon energies of 75 and 230 MeV. Measurements were made mostly at 90° in the center-of-mass system, but limited data at 45° and 135° were also obtained. The data below 140 MeV are compared with current theories. At 90° our results are generally smaller than theoretical calculations. The measured asymmetry changes sign at about 130 MeV and shows a backward peaking at the higher energies.

I. INTRODUCTION

PHOTODISINTEGRATION of the deuteron has been extensively studied from threshold energy to several hundred MeV and a comprehensive bibliography is now available.[1] The photodisintegration process may be divided roughly into two energy regions, one below the pion-production threshold and one above this threshold. At energies below pion threshold, viz.,

* Work supported in part by the U. S. Office of Naval Research, the U. S. Atomic Energy Commission and the U. S. Air Force Office of Scientific Research.

[1] Bibliography of photonuclear and electronuclear disintegrations compiled by M. E. Toms, July 1963, U. S. Naval Research Laboratory.

about 140 MeV, the photodisintegration process is dominated by direct radiative interaction of the photon with the proton as a rigid, charged particle. At energies above the pion threshold, explicit reference to pion physics is required in order to obtain even a qualitative understanding of the total cross section.[2]

Below the pion threshold, there are many theoretical calculations of varying complexity.[1] Partovi's recent calculations[3] fit the total cross section rather well up to about 100 MeV, but above this energy, the cross section is larger than calculated. His fit to the angular distribution is also good up to about 100 MeV. The main attempts in the analysis of this elementary photodisintegration process below the pion threshold have been to understand the nature of the interaction between the electromagnetic field and the nucleus, or inversely, assuming this interaction is known, to derive some knowledge about the deuteron. This dual approach has been fruitful in evaluating the relative importance of the multipole fields in the interaction, the D-state probability of the deuteron, and the final-state interaction of the n-p system. In all previous experiments, unpolarized bremsstrahlung was used as a source of photons. By employing polarized photons as in the present experiment, knowledge about the dynamics and electromagnetic properties of the two-nucleon system is further tested.

There are indications that even at energies below 130 MeV, virtual-pion effects may be present,[2] but at energies above this threshold, production and reabsorption of pions show up unambiguously. There is no comprehensive theory available as in the lower energy region, but there are some models to explain the magnitude of the total cross section. For instance, Wilson[4] assumed that a pion is produced from one of the nucleons of the deuteron and then subsequently reabsorbed by the other nucleon. The asymmetry measurement should shed further light on the dominant mechanism at these energies.

Section II describes the experimental details and data analysis, while in Sec. III the experimental results are presented and discussed.

II. EXPERIMENTAL PROCEDURE

A. Polarized Photon Beam

The Stanford Mk III linear accelerator was used to produce a polarized bremsstrahlung beam. This technique of producing a polarized photon beam by selection of the off-axis bremsstrahlung was first described by Taylor and Mozley,[5] and subsequently investigated in more detail by Mozley and others.[6] The present polarized photon beam was obtained by the same technique. The percentage polarization of the photon beam reaches a maximum at an angle of $\alpha=mc^2/E_0$ to the electron-beam direction, where E_0 is the energy of the electron beam and m the mass of the electron. After multiple scattering and aperture fold, a maximum polarization of photon beam is reached at about 1.25 mc^2/E_0. The percentage polarization of the photon beam is a function of k/E_0, where k is the photon whose polarization is desired. The smaller this ratio the higher the percentage polarization. Therefore, for any photon energy, it is desirable to use an electron beam of maximum allowable energy as determined by other considerations. The main condition is the requirement that the detected proton be uncontaminated by those from the recoil of the single-pion production. This limitation is particularly important at forward angles, as shown later.

The electron beam was monitored with a secondary emission monitor and the photon beam by a hydrogen-flow ionization chamber. Since only ratios of the counting rates were measured, the sole requirements on these monitors were that they should be reproducible at any electron-beam energy and intensity, at which the experiments were run. No efforts were made to determine the efficiency or the energy response of these monitors. The saturation effect was, however, checked and found to be insignificant at our beam intensity. The problem of measuring photon flux, a source of error in photon experiments, was also avoided since only ratios were taken.

B. Experimental Details

The experimental layout is shown in Fig. 1. This arrangement was essentially the same as in Ref. 6. The length of the liquid-deuterium target cell was 10 in. but the effective length as seen by the spectrometer was smaller and varied with the angle of the spectrometer. A dummy cell, either empty or filled with liquid hydrogen was used for background measurements. The counter system consisted of three $4\times4\times\frac{1}{16}$-in. plastic scintillators placed in the focal plane of the spectrometer, giving three momentum channels of approximately 3% each. Each one of the three momentum-defining counters was placed in coincidence with another plastic scintillator backing counter. The protons were distinguished from the electrons and meson backgrounds by their pulse heights in these counters. The associated electronic circuits were transistorized and were very stable in operation. The dead time of the discriminator was measured to be about 30 nsec and the resolving time of the coincidence circuit was about 10 nsec so that at the singles rates of approximately 2/sec the

[2] G. R. Bishop and Richard Wilson, *Handbuch Der Physik*, edited by S. Flügge (Springer-Verlag, Berlin, 1957), Vol. 42, pp. 309–361.
[3] F. Partovi, Physics (N. Y.) **27**, 79–113 (1964).
[4] R. R. Wilson, Phys. Rev. **104**, 218 (1956); B. Feld, Nuovo Cimento, Vol., II, Suppl. 2, 145, (1955); N. Austern, Phys. Rev. **100**, 1522 (1955); F. Zachariasen, *ibid.* **101**, 371 (1956).
[5] R. E. Taylor and R. F. Mozley, Phys. Rev. **117**, 835 (1960).
[6] R. C. Smith and R. F. Mozley, Phys. Rev. **130**, 2429 (1963); D. J. Drickey and R. F. Mozley, *ibid.* **136**, B543 (1964).

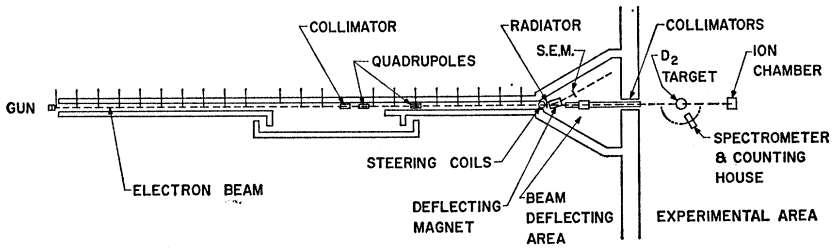

FIG. 1. The experimental layout.

dead-time and chance-rate corrections were negligible. For the points above 200 MeV at 45° and 90° in the c.m. system, copper absorbers of thickness $\frac{1}{2}$ and $\frac{1}{4}$ in, respectively, were placed in front of the spectrometer entrance to degrade the proton momentum. This increased the energy spread of the data, but did not affect the results otherwise.

For each datum, the energy of the electron beam was chosen to be as high as feasible, so as to obtain maximum polarization of the photon beam. This choice of the electron-beam energy was determined by kinematics and background considerations, as discussed in the next section. The procedure of data collection was as follows: The well collimated monochromatic beam of the linear accelerator was steered and focused on a phosphorescent screen in the beam pipe of the accelerator. The beam spot was in general elliptical in shape and less than 0.25 in. in the largest dimension. The screen was then replaced by a 0.003-in. aluminum radiator and the photon beam centered about a copper collimator situated about 400 in. away as shown in Fig. 1. The copper collimator was 8 in. long and $\frac{7}{16}$ in. in diameter. The electron beam was then deflected by means of Helmoltz coils immediately before it struck the radiator, the angular deflection being adjusted to be $1.25\ mc^2/E_0$. The beam was first deflected horizontally right, vertically down, horizontally left, and then vertically up. We denote these positions by R, D, L, U, respectively. Figure 2 shows schematically the portions of the bremsstrahlung beam intercepted by the collimator. The length of the vector $N_\perp$ represents the number of photons whose electric vector is perpendicular to the photon-emission plane and the length of the vector $N_{\parallel}$ represents the number of photons whose electric vector is parallel to this plane. The polarization of the photon beam is then given by[6]

$$P=(N_\perp-N_{\parallel})/(N_\perp+N_{\parallel}).$$

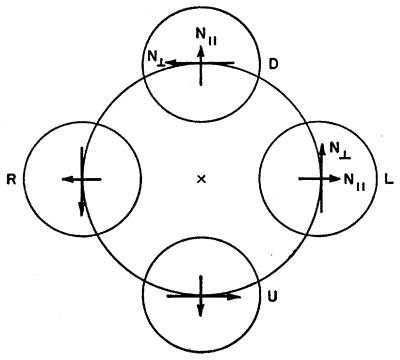

FIG. 2. The collimated portions of the bremsstrahlung beam for the indicated deflected positions of the electron beam.

At each position of deflected electron beam, it was allowed to remain for a time long enough for a fixed amount of charge to be collected by the ionization chamber. The beam was then deflected to the next position. The cycling usually started from position R and automatically stopped at a preset number of cycles. At each position, the electron beam in general remained for only a few minutes. The counts from the scintillators were routed so that at beam positions R and L, these counts were stored in one place, denoted by $R+L$ and when the beam was at the positions D and U, the counts were stored at another place. The measured asymmetry was given by

$$A=\frac{(R+L)-(D+U)}{(R+L)+(D+U)}.$$

The cycling procedure minimized the effect of inaccurate beam centering which was also checked by auxilliary circuits storing the combinations $R+D$, $L+U$, $R+U$, $L+D$. These "asymmetry ratios" therefore served as a check; for example, the ratio

$$\frac{(R+D)-(L+U)}{(R+D)+(L+U)}$$

would measure beam centering about the 45° axis and was in all cases consistent with zero. This gave us confidence in our measurement of A for that run.

At the end of a night's run, the electron beam was passed through a 0.0015 in. aluminum radiator and a glass-slide picture of the beam at the position of the collimator was taken.[6] The distribution of the electrons on the glass slide provided information for the calculation of polarization of the photon beam. The calculated values of polarization of the photon beam for a typical electron-beam size is shown in Fig. 3.

C. Kinematic Considerations and the Photon-Energy Determination

Photodisintegration of the deuteron is a two-body process, so that by selecting the angle and the momentum of the proton in the laboratory system, the energy

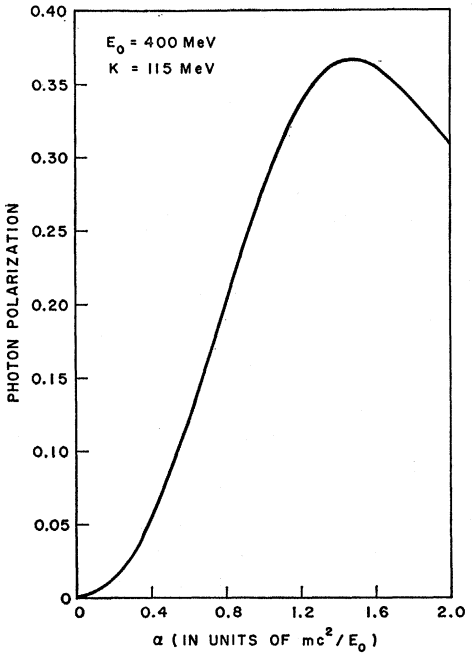

FIG. 3. The calculated polarization of the photon beam. The energy of the electron beam is 400 MeV. α is the angle between the electron-beam axis and the collimator center.

of the photon initiating the disintegration is uniquely determined. The solid line in Fig. 4 shows the momentum of the proton as a function of the emission angle in the laboratory system for various photon energies. The dash-dotted lines show the kinematic relationship of the recoil protons from single-pion photoproduction. These protons may be confused with those from the disintegration process at lower photon energies, unless care is taken in the choice of the electron-beam energy. In the above case, the other nucleon is treated as a spectator and contributes nothing to the process. This is evidently one limiting case and is by far the most important, as shown in the excitation function. In the other extreme case, the other nucleon and the pion recoil as a whole giving maximum momentum to the proton. The kinematics for this case are shown by the dashed lines. This process is more difficult to eliminate without greatly reducing the polarization of the photon beam. Fortunately, this process is not very important and introduces a negligible contamination as shown experimentally both in the excitation function and in the asymmetry measurement at 80 MeV, where the situation was the worst.

As is evident from the above kinematic considerations, the measurements at 90 and 135° in the c.m. system are free from single-pion production contamination for reasonably high electron-beam energy. For all these points, the electron beam energy was chosen to be 400 MeV. With this value of the end point of the bremsstrahlung beam, there was still the possibility of contamination of protons from the other extreme case of single-pion production as mentioned earlier. This contamination was, however, checked for each point in the excitation function, and found to be negligible within the statistical accuracy of our data.

The limitation on the electron-beam energy in the forward angles was much more severe as evident from Fig. 5. We investigated this contamination by measuring an excitation curve for deuterium and hydrogen targets. Proton counts were obtained for a fixed reading of the ionization chamber at progressively decreasing electron beam energies, the spectrometer being set at a fixed momentum and angle. The excitation function obtained at 115 MeV, 39.5° in the laboratory system is shown in Fig. 5. The shape of the excitation function is a fold of the bremsstrahlung spectrum, the spectrometer resolution function and the differential cross section. The contribution from the single pion production in Fig. 5 is clearly indicated by the rise starting at approximately $E_0 = 250$ MeV. For this datum, the electron beam was set at 220 MeV.

The accuracy of photon-energy determination was estimated at 2%.

D. Backgrounds and Checks

The proton contamination at each point due to single-pion production was determined by using a liquid-hydrogen target instead of the regular liquid-

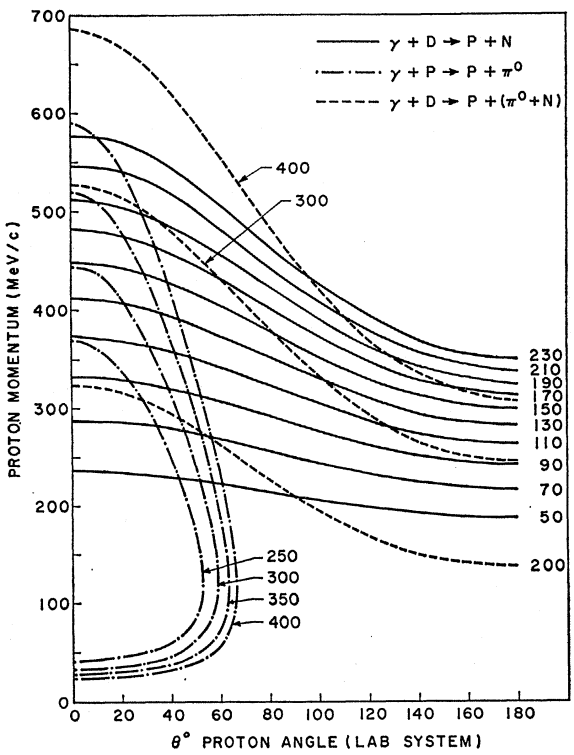

FIG. 4. The kinematics for photodisintegration of the deuteron. The two extreme cases in the kinematic relationship of single-pion production from a single nucleon are also shown.

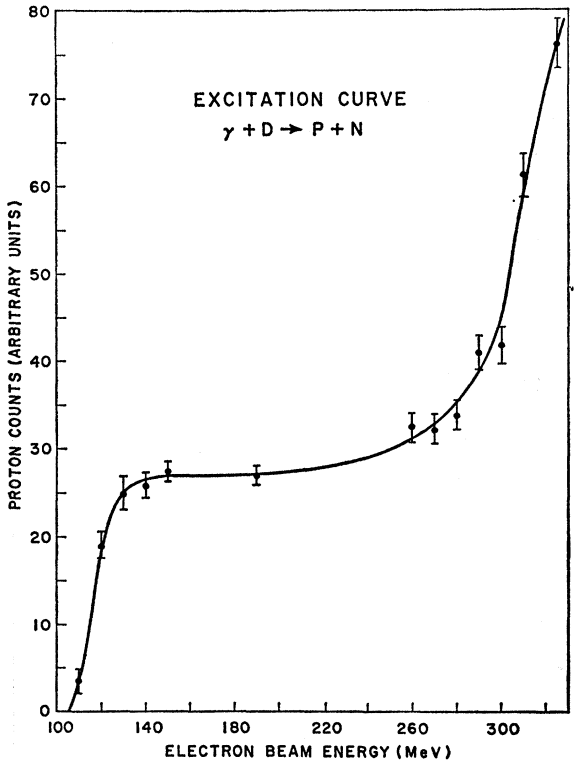

FIG. 5. The excitation function at $K=115$ MeV, 39.6° proton recoil angle in the laboratory. Single π^0 production is clearly noticeable above 250 MeV.

deuterium target. At the electron-beam energy chosen to produce the bremmstrahlung, the contamination produced in each point was found to be zero within statistics. The pulse-height spectrum of the plastic scintillator counters were displayed in a pulse-height analyzer and the high voltage on the photomultiplier tubes was adjusted so that only heavily ionizing particles were counted. The pion contamination in the spectrum was experimentally determined in each case by reversing the magnetic field of the spectrometer, and was generally less than 2%. The empty-target background was found to be negligible. The no-radiator background varied slightly from run to run, but was usually less than 5%. The backgrounds from the no-radiator bremsstrahlung, empty-target, reverse-magnetic-field and hydrogen-target runs were subtracted when they were larger than 1%. The toroid signal of the electron beam showed that the electron beam was in general about 1 μsec in duration. The counting-rate correction was negligible.

As a check on the asymmetry measurement, a point was taken with the electron beam deflected at 45° to the horizontal plane and there was no asymmetry in the proton counts within statistics. A continuous monitoring on the centering of the photon beam was afforded by simultaneously storing the data in such a manner as to check it as indicated earlier. The sign of the measured asymmetry was also compared in a separate run with that from single-neutral-pion production which has a large positive asymmetry at the first resonance, since this process is dominated by $M1$ transitions.[6]

III. DATA ANALYSIS

In the energy region below 130 MeV, the differential cross section by unpolarized photons can be written as[7]

$$\sigma_0(\theta)=a(1+\beta_1\cos\theta)+b(1+\beta_2\cos\theta)\sin^2\theta. \quad (1)$$

If the photon beam is polarized with polarization P, then the differential cross section will have an azimuthal dependence given by

$$\sigma(\theta)=\sigma_0(\theta)[1+P\Sigma(\theta)\cos 2\chi], \quad (2)$$

where χ is the angle between the electric vector of the photon and the production plane of the proton. The asymmetry function Σ provides extra information which is not available by the use of unpolarized photons only.

When the electron beam was deflected to L or R as indicated in Fig. 2, the number of proton counts was given by

$$N'=C\sigma_0[1-P\Sigma], \quad (3)$$

where C is a constant, dependent on the solid angle, monitor response, target thickness, counter efficiencies, etc., which were not relevant to the ratio. Similarly, when the electron beam was deflected to D or U, the number of counts was given by

$$N=C\sigma_0[1+P\Sigma]. \quad (4)$$

The measured asymmetry was then given by

$$A=(N'-N)/(N'+N)=-P\Sigma. \quad (5)$$

The polarization of the photon beam is defined as a positive number,

$$P=(N_\perp-N_{\parallel})/(N_\perp+N_{\parallel})$$

thus making the sign of measured asymmetry A negative, if the proton tends to be produced more copiously along the electric vector.

In general, it is possible to write[3]

$$\sigma_0(\theta)\Sigma(\theta)=\sin^2\theta\sum_{n=0}^{L}a_n\cos^n\theta, \quad (6)$$

where L is an integer determined by the multipolarity of the transition. The coefficients a_n are, of course, energy-dependent. If only $E1$, $M1$, and $E2$ transitions are considered, we have

$$\sigma_0(\theta)\Sigma(\theta)=\sin^2\theta(a_0+a_1\cos\theta). \quad (7)$$

The expression for Σ is particularly simple at 90°

[7] J. J. DeSwart, Physica **25**, 233 (1959). J. J. DeSwart and R. E. Marshak, *ibid* **25**, 1001 (1959).

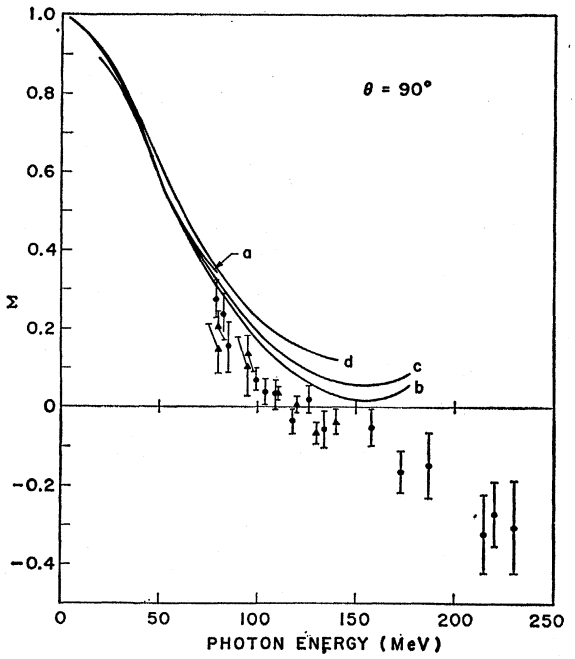

FIG. 6. Σ, the asymmetry function, at 90° in the c.m. system. Curve a is that of Ref. 7, b and c are from Ref. 8, and d is from Ref. 3, approximation *I*.

in the c.m. system[7]

$$\Sigma(90°)=((b_e-b_m)/(b_e+b_m))(1/1+(a/b)), \quad (8)$$

where the differential cross section is written as $\sigma_0=a+b$ as in Eq. (1) and $b=b_e+b_m$, the subscripts denoting the electric and magnetic parts, respectively. In Partovi's work, an expansion in $\cos\theta$ to second order was used, and a simple separation as shown in expression (8) was not possible.

The asymmetry function Σ was calculated by DeSwart[7] in the energy range from threshold to 80 MeV. Assuming only $E1$, $M1$, and $E2$ transitions, we used expression (8) to evaluate Σ from the amplitudes given in Ref. 8, in their approximations B and C, which include $E1$ and $M1$ transitions only. The recent work of Partovi also gave the asymmetry function. These theoretical calculations are shown in Fig. 6. The curve labeled a is taken from Ref. 7, b and c are from Ref. 8, and d is taken from Ref. 3, approximation *I*. The experimental values are also plotted for comparison. The errors are due to statistics only. Some of the experimental values shown in triangle were reported earlier.[9]

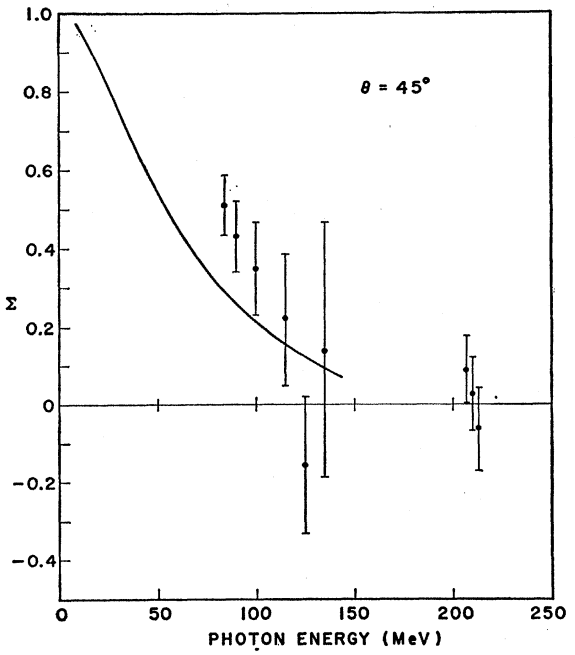

FIG. 7. Σ, the asymmetry function, at 45° in the c.m. system. The fit is that of Partovi.

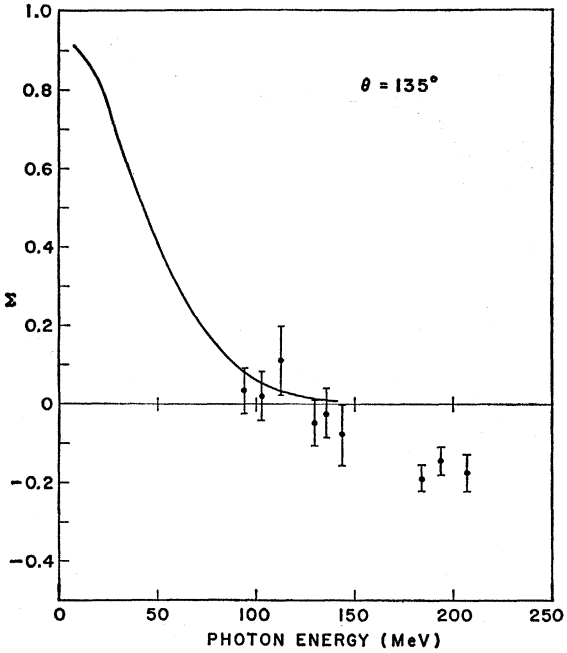

FIG. 8. Σ, the asymmetry function, at 135° in the c.m. system. The fit is that of Partovi.

The experimental values at 45 and 135° in the c.m. system are shown in Figs. 7 and 8, respectively. The fits shown are calculated by Partovi in his approximation I.

IV. DISCUSSION

The results can best be discussed in terms of two energy regions, one below pion threshold and one above. For the region below the pion threshold, the asymmetry function Σ has been calculated by various authors.[3,7,8]

[8] M. L. Rustgi, W. Zernik, G. Breit, and D. J. Andrews, Phys. Rev. **120**, 1881 (1960).
[9] F. F. Liu, Physics Letters **11**, 306 (1964).

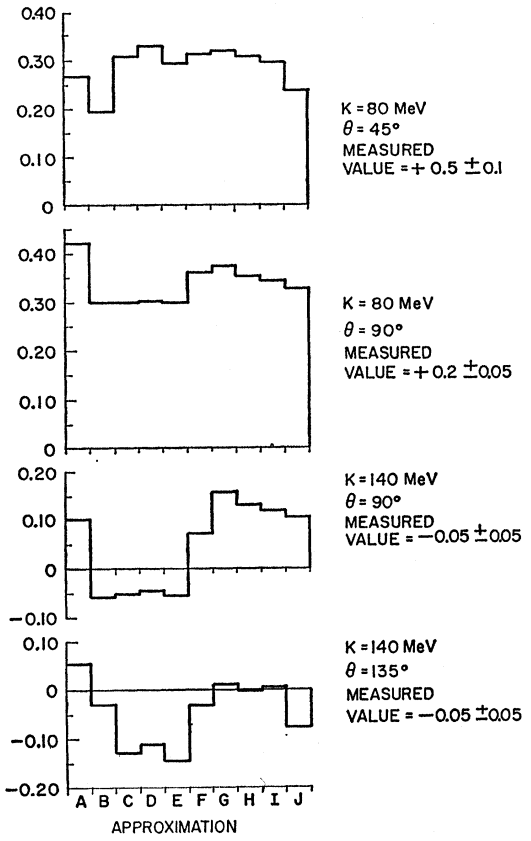

FIG. 9. Successive approximation of Σ as calculated by Partovi.

We shall, however, compare our data chiefly with respect to the calculation by Partovi, although other calculations are also shown in the figures. Partovi has attempted the most complete nonrelastivistic, phenomenlogical treatment of the problem. The various assumptions and approximations are stated in his work, to which the reader is referred for details.

In Fig. 9, we have plotted the values of Σ for the various approximations (*A*-*J*) as calculated by Partovi. In approximation *A*, only *E*1 transition is considered. This is clearly not in accord with the experimental results at 90°. Moreover, the differential-cross-section measurements at 80 MeV clearly indicated the presence of other transition amplitudes. In approximation *B*, singlet *M*1 transitions have been included in addition to *E*1. The fit is substantially improved although complete agreement is not obtained. Approximations *C*, *D*, *E*, are in qualitative agreement with the results, but paradoxically the approximations *F*, *G*, *H*, *I* or *J* give poorer fits. This would therefore tend to cast some doubt on the validity of multipole treatments that exclude meson effects.

The fits in Figs. 6, 7, and 8 are those of approximation I, this being the result of the most complete calculation. The data at 90° are substantially lower than the theoretical value. In order to bring the data into agreement, we would have to decrease the percentage polarization of the photon beam by about 50% of the calculated one. A systematic error of this magnitude is rather unlikely, in view of the results of other experiments.[6] Data were taken at other angles to give us a rough idea of the angular distribution. They were limited at the forward angles by the momentum range of the spectrometer, and kinematics as mentioned earlier and at backward angles by the limited range of the emitted proton. Because of the limited nature of the angular distribution, very little can be said about it.

In the energy region above pion threshold, the most obvious feature of the data is the change in sign of the asymmetry. This change in sign seems to occur at approximately 140 MeV at all angles. At present there is no theoretical calculation of this asymmetry at these energies. As mentioned before, the total cross section in this energy range cannot be explained without recourse to meson physics. It is also clear from the above considerations that any calculation of Σ will have to introduce the pion explicitly.

It is of interest to note that in this high-energy region, the angular dependence of the asymmetry function Σ is peaked in the backward hemisphere. This reminds one of the very pronounced forward peaking of the differential cross section at these same energies.

ACKNOWLEDGMENTS

The author wishes to thank Dr. R. F. Mozley for his continued support and many helpful discussions. E. Maninger and R. Zdarko were very generous with their help in taking the data. The author also wishes to thank the accelerator-operating personnel under Dr. P. Wilson for their efficient cooperation.